Reduction of the Jahn-Teller distortion at the insulator-to-metal transition in mixed valence manganites

J. L. García-Muñoz, M. Suaaidi, and J. Fontcuberta
Institut de Ciència de Materials de Barcelona, Consejo Superior de Investigaciones Científicas Campus, Universitat Autònoma de Barcelona, Bellaterra 08193, Spain

J. Rodríguez-Carvajal
Laboratoire de Leon-Brillouin (Commissariat à l'energie atomique-Centre National de la Recherche Scientifique), Centre d'Etudes de Saclay, 91191 Gif sur Yvette Cedex, France

(Received 11 April 1996)

The insulator-to-metal transition in the manganite $La_{0.52}Y_{0.15}Ca_{0.33}MnO_3$ ($T_{IM}\approx 115$ K) has been studied by high-resolution neutron powder diffraction. The cell volume contraction at the Curie point is accompanied by a remarkable decrease of the Jahn-Teller distortion in MnO_6 octahedra. The change of the Mn-O bond lengths at T_{IM} is anisotropic and brings about a drop out of the basal-plane collective distortion mode Q_2, proposed to be the deformation responsible for the band split of $e_{g\uparrow}$ orbitals. This is consistent with the double-exchange picture, and precludes simple ferromagnetic exchange. [S0163-1829(97)08648-1]

The electronic structure and exchange interactions in transition-metal perovskites was a controversial topic many years ago.[1] To this group of materials belong the perovskite-based $Ln_{1-x}A_xMnO_3$ (A=Ca, Sr, Ba) compounds which exhibit a large negative colossal magnetoresistance (CMR) at temperatures close to the sharp peak in the resistivity (T_{IM}).[2] There is a drastic change in the dynamics of Zener electrons connected with the resistivity peak: the electrical conductivity changes up to 10^6%, the change being a maximum for concentrations near $x\approx\frac{1}{3}$.[2] Several striking features make this transition extraordinarily attractive: it has been shown, for instance, that it separates two regions in which the resistivity is, respectively, described by $\rho(T)\sim\exp(T_0/T)^{1/4}$ ($T>T_{IM}$) and $\rho(T,H)\sim\exp\{-[M(T,H)]\}$ ($T<T_{IM}$) (M, magnetization).[3,4] In addition, intriguing magnetoelastic effects have also been observed associated with the appearance of ordered moments.[5,6] One of the most relevant issues, then, to be investigated in these fascinating manganese perovskites is the physical origin of the large change in electron mobility observed at the transition.

Two different distortions characterize the pervoskite structure of mixed manganites: (a) one is the cooperative tilt of MnO_6 octahedra, common in all ABO_3 perovskites, with origin at the ''free space'' left out in the structure by small Ln atoms (the so called O-type structure, with $a\leqslant c/\sqrt{2}\leqslant b$ for orthorhombic $Pbnm$ perovskites). The size of Ln atoms modifies the bending of the Mn-O-Mn bond angle (θ), the strength of the hopping integral between e_g (Mn)-p_σ(O)-e_g (Mn) orbitals and, therefore, the electronic bandwidth.[4,7] (b) The second is related to the strong Jahn-Teller character of trivalent manganese in the octahedral sites, due to its $3d^4{:}t_{2g}^3e_g^1$ electron configuration.[1] The anomalous distortion observed in $LaMnO_3$, compared to $LaCrO_3$ or $LaFeO_3$ with the oxygen octahedra severely deformed, is known to be due to a frozen-in Jahn-Teller (JT) distortion with long-range order at the wave vector (π,π,π).[8] In the ideal cubic case $LaMnO_3$ would be metallic with the Fermi energy lying in the middle of the $e_{g\uparrow}$ bands. A JT distortion of the Q_2 type (antiferrodistorsive), that displaces the basal plane oxygen

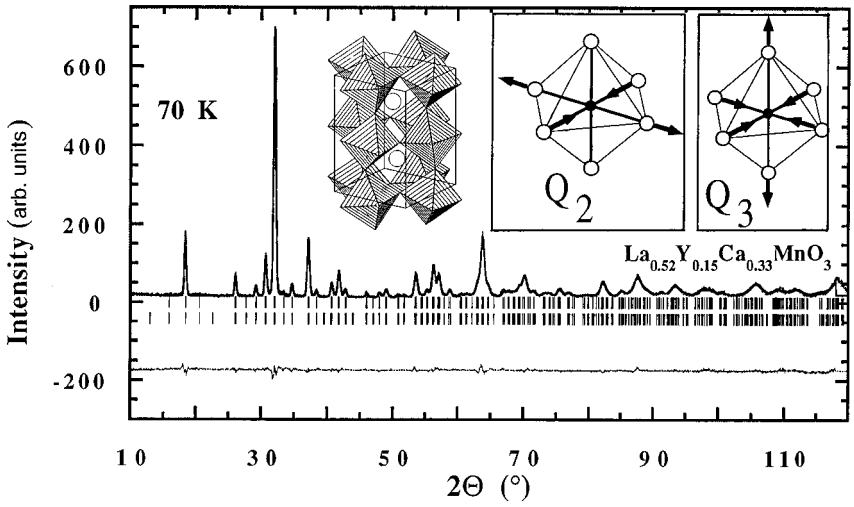

FIG. 1. Observed (+) and calculated (−) neutron diffraction patterns for $La_{0.52}Y_{0.15}Ca_{0.33}MnO_3$ at 70 K. The second row of markers labels magnetic reflections. Inset: crystal structure of $La_{0.52}Y_{0.15}Ca_{0.33}MnO_3$ and some of the main collective distortion modes of the octahedron.

atoms from their ideal positions (see Fig. 1), has proposed to be responsible for the insulating state.[1,9] This distortion does not change the lattice symmetry ($Pbnm$) but modifies the cell deformation in such a way that $c/\sqrt{2} \leqslant a \leqslant b$ (the O'-type structure). Thus, the resulting Mn-O bond lengths of 1.918 and 2.145 Å (basal plane) and 1.973 Å (apical distance) at room temperature[10] are at the origin of a small gap between the JT split Mn e_g bands ($d_{x^2-y^2}$ and $d_{3z^2-r^2}$ like) in pure $LaMnO_3$. The JT split of the e_g band is progressively reduced as Ca concentration increases in the intermediate $La_{1-x}Ca_xMnO_3$ compounds.[11] As a consequence the distortions are reduced with x in $La_{1-x}Ca_xMnO_3$ (Ref. 11) due to the fact that the driving force for the JT distortion is reduced. For these intermediate compounds, the $e_{g\uparrow}$ electrons hop among different Mn positions propagating the correlation effects associated with the intra-atomic ferromagnetic coupling (Hund) between localized $t_{2g\uparrow}$ spins and partially delocalized $e_{g\uparrow}$ electrons [double exchange (DE)]. This originates ferromagnetic clusters that can be viewed as ferromagnetic polarons. There are indications that the localized polaron picture holds also below T_{IM} (Ref. 3) and that the $e_{g\uparrow}$ electrons are weakly localized in large wave packets. As evidenced by Matsumoto,[11] below T_{IM} a dynamic JT effect and slowly fluctuating local JT distortions also tend to localize the Zener electrons as polarons. The actual knowledge of what determines the different carrier dynamics below and above T_{IM} is still very scarce. In this paper we present the results of a high-resolution neutron-powder-diffraction study on $La_{0.52}Y_{0.15}Ca_{0.33}MnO_3$, which provides direct experimental evidence of a notable reduction of the local JT distortion at T_{IM}. We will show that the reconfiguration of the oxygen positions around Mn ions implies *the disappearance of the basal-plane distortion mode* Q_2, proposed to be the deformation responsible for the $e_{g\uparrow}$ band split in the pure compound. The present results give evidence of a true electronic reorganization at T_{IM} different from a single isotropic bond contraction. In addition, the changes observed in the basal-plane symmetry of MnO_6 octahedra, from rhombic to tetragonal, clearly support the DE model against the simple ferromagnetic exchange.

Neutron diffraction data were obtained on a well-characterized polycrystalline sample of $La_{0.52}Y_{0.15}Ca_{0.33}MnO_3$ at the Reactor Orphèe of the Laboratoire Léon-Brillouin. High- and medium-resolution 3T2 and G4.1 powder diffractometers were used ($\lambda = 1.227$ and 2.426 Å, respectively) between 1 K and room temperature (RT). Details about sample preparation have been reported in Ref. 4, and previous characterization involved x-ray diffraction, magnetic and magnetoresistivity measurements.[4,12] The sample was single phase and its cationic stoichiometry was determined to be nominal (± 0.01) by analysis of the neutron diffraction data. The oxygen content was found to be 3.00 within the calculated standard error (1%). We performed Rietveld refinements of the nuclear and magnetic structures of neutron data using the program FULLPROF.[13] When orthorhombic ($Pbnm$) $La_{0.52}Y_{0.15}Ca_{0.33}MnO_3$ is cooled, the resistivity peak at ≈ 115 K signals the I-M transition, whereas ordered moments are already visible below $T_c \approx 140$ K, simultaneously to the onset of structural anomalies.

From high-resolution measurements at 300, 140, and 70 K (the last two, respectively, above and below the I-M transition), selected bond lengths, angles, and isotropic thermal parameters are gathered in Table I. Figure 1 shows, as example, the fitted neutron diffraction pattern at 70 K. In Fig. 2(a) the cell volume shows a contraction coinciding with the onset of ordered moments [see also Fig. 2(c)]. In this sample the maximum in the resistivity (T_{IM}) does not coincide exactly with the onset of partial moment ordering (T_C), a signature of persisting large magnetic clusters beyond T_{IM}.[4] The lattice contraction observed ($\Delta V/V \approx 0.15\%$) is a consequence of the lattice parameter variation shown in Fig. 2(b). The main change corresponding to the b axis $\Delta b/b \approx 0.11\%$.

TABLE I. Selected structural and thermal parameters, interatomic distances (Å) and angles (deg) for $La_{0.52}Y_{0.15}Ca_{0.33}MnO_3$ from neutron diffraction data ($T_{IM} \approx 115$ K).

	N	70 K	140 K	300 K
a (Å)		5.4404(5)	5.4416(5)	5.4500(4)
b (Å)		5.4603(5)	5.4661(5)	5.4685(5)
c (Å)		7.6863(6)	7.6884(6)	7.6965(6)
V (Å^3)		228.33	228.68	229.38
$d_{\text{Mn-O(1)}}$	2	1.956(1)	1.954(1)	1.958(2)
$d_{\text{Mn-O(2)}}$	2	1.963(2)	1.964(2)	1.959(2)
$d_{\text{Mn-O(2)}}$	2	1.963(2)	1.967(2)	1.972(2)
d_{equat}		1.963(2)	1.965(2)	1.965(2)
$\langle d_{\text{Mn-}O} \rangle$		1.960(2)	1.961(2)	1.963(2)
θ_1	2	1.58.6(3)	159.2(3)	158.5(3)
θ_2	4	158.2(7)	157.7(8)	158.3(7)
$\langle \theta \rangle$		158.3(6)	158.2(6)	158.4(6)
$\left(\frac{d_{\text{equat}}}{d_{\text{apical}}} - 1\right) \times 10^4$		36	58	38
$\Delta_d 10^4$		0.028	0.081	0.105
MnO_6 octahedra				
O(1)-Mn-O(2)	2	89.5(3)	88.7(3)	88.7(3)
O(1)-Mn-O(2)	2	90.2(3)	91.3(3)	91.2(3)
O(2)-Mn-O(2)	2	90.9(3)	90.9(3)	90.9(3)
Thermal parameters				
B_{Ln} (Å^2)		0.42(5)	0.58(5)	0.74(5)
B_{Mn} (Å^2)		0.19(5)	0.20(5)	0.25(6)
$B_{\text{O(1)}}$ (Å^2)		0.62(6)	0.86(6)	0.92(7)
$B_{\text{O(2)}}$ (Å^2)		0.74(5)	0.84(5)	1.06(5)

Concentrating first on the high-temperature phase (see Table I), we observe a ''permanent'' or ''static'' distortion above T_C that results in octahedra with two different Mn-O(2) distances in the basal [1.959(2), 1.972(2) Å] and an apical distance Mn-O(1)=1.958(2) Å (at 300 K). One can thus assume that, as in $LnMnO_3$ oxides, the static JT component in the paramagnetic phase is described by the combination of the following collective modes: the breathing mode Q_1, the octahedral stretching mode Q_3, and Q_2, the mode displacing the O(2) oxygens in the two basal-plane diagonals, respectively, closer and farther to the center of the MnO_4 square (see inset of Fig. 1).

The first key observation, then, is that the static distortion found can be considered ''reminiscent'' of that existing in the undoped compound since it is of the same type,[9,10] but the magnitudes of the oxygen displacements have been se-

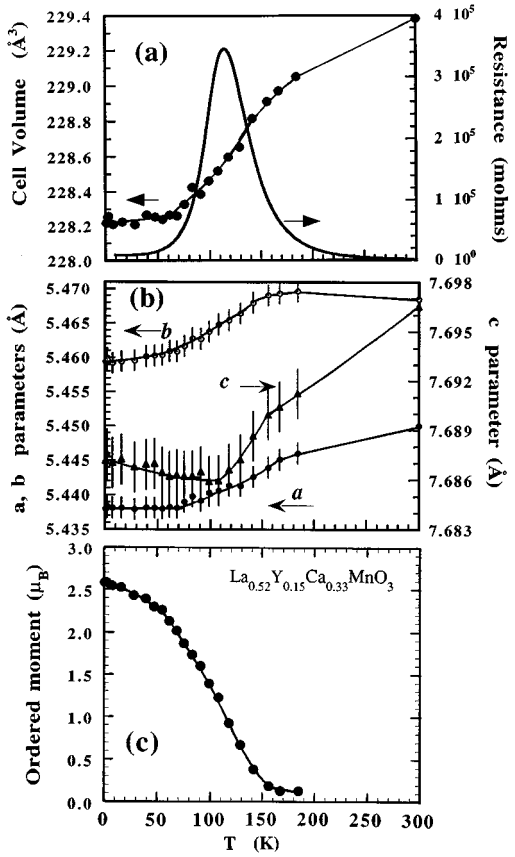

FIG. 2. (a) Temperature dependence of the unit-cell volume for $La_{0.52}Y_{0.15}Ca_{0.33}MnO_3$ showing the contraction at T_c. For comparison the electric resistivity vs T is also shown. (b) Thermal evolution of lattice constants. (c) Thermal evolution of the ordered ferromagnetic moment at the Mn.

verely reduced in the $x=\frac{1}{3}$ compound. This is, therefore, a strong indication of a ''reminiscent'' JT static deformation. In this respect, it is noteworthy that according to our data this manganite is of O' type in all the temperature range, thus reinforcing an active JT distortion. Compared to $La_{2/3}Ca_{1/3}MnO_3$, the enhanced Mn-O-Mn bending in $La_{0.52}Y_{0.15}Ca_{0.33}MnO_3$ leads to a narrower $\sigma^*(e_{g\uparrow})$ bandwidth,[4] the kinetic energy of the Zener electrons is thus reduced and the JT mechanism favored.[14]

A similar unusual cell contraction was observed at the thermally driven insulator-to-metal transition in isostructural $LnNiO_3$ perovskites.[15] However, in spite of their similarities, we will show in the following that there are significant differences in the manganite that point towards a rearrangement of the electronic ground state supported by modifications in the Jahn-Teller distortion. In the transition to the metallic state in $LnNiO_3$,[15] there is a discontinuous isotropic contraction of the Ni-O bonds [$\Delta d_{\text{Ni-O}} \approx -0.004(1)$ Å] that causes a contraction of the octahedron and coupled tilts of the NiO_6 units ($\Delta\theta_{\text{Ni-O-Ni}} \approx 0.5°$). In sharp contrast, the structural accommodation in $La_{0.52}Y_{0.15}Ca_{0.33}MnO_3$ has the following microscopic relevant features: (i) The basal-plane distortion progressively vanishes and the displacement of the O(2) atoms results in *identical Mn-O*(2) *equatorial distances* [$d_{\text{Mn-O(2)}} \approx 1.963(2)$ Å]. (ii) The largest bond-length contraction at T_{IM} corresponds to the long Mn-O(2) bond for

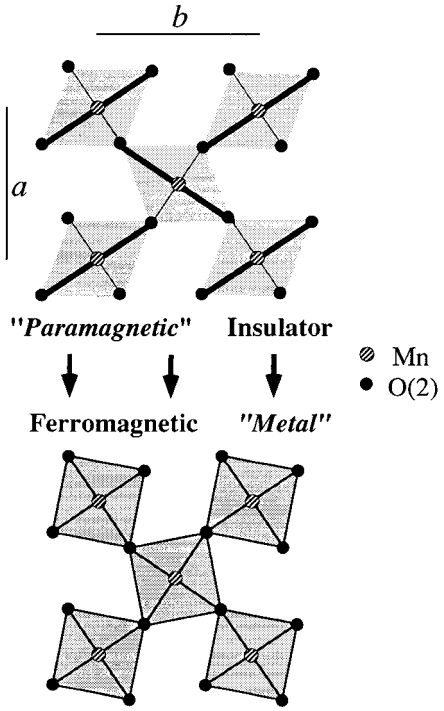

FIG. 3. Schematic drawing of the structural anomalies in ab basal planes accompanying the I-M transition.

which $\Delta d_{\text{Mn-O(2)}} \approx -0.004(2)$ Å. (iii) At the same time the apical Mn-O(1) bond is slightly expanded [$\Delta d_{\text{Mn-O(1)}} \approx 0.002(1)$ Å] with respect to its high-temperature value.

As a result, the above modifications bring about a more ideal MnO_6 octahedron in the ferromagnetic phase. This is further confirmed by the changes in the O-Mn-O angles defining the octahedron, measured above and below T_{IM} (see Table I). Essentially, the O(2)-Mn-O(2) angle has the same values between 70 and 300 K, but a very different behavior exhibited by the two angles subtended by apical O(1) oxygens and equatorial O(2) atoms. As a result, respectively, they bend and straighten out by about 1° towards the ideal value of 90° when entering the metallic regime. Moreover, by considering the mean distortion in the MnO_6 octahedra Δ_d ($\Delta_d = (1/N)\Sigma_{i=1}^{N}[(d_i - \langle d\rangle)/\langle d\rangle]^2$), Table I shows that its value is decreased by a factor 3 below T_{IM}.

So far, we have demonstrated a reduction in the JT distortion at the transition. Physically, it means that carrier delocalization results in a weaker electron-phonon coupling, and this weakens the driving force for JT distortion. Now we concentrate on key aspects of the magnetic coupling in these systems. Goodenough[1] and Kanamori,[8] first and, recently, Refs. 9–11 have discussed the superexchange mechanism of $LaMnO_3$ based on the ground-state hole wave function $d_{x^2-y^2}$. In undoped manganites the ferromagnetic planes derive from occupied Mn $d_{3z^2-r^2}$ orbitals alternatively pointing along [110] and [$\bar{1}$10] directions, coinciding with the long Mn-O(2) bond (see Fig. 3). Hence, the ferromagnetic coupling is determined by the exchange interaction between the empty $d_{x^2-y^2}$-p_σ orbitals and the occupied $d_{3z^2-r^2}$-p_σ band. From the present results, the onset of long-range ferromagnetism in $La_{0.52}Y_{0.15}Ca_{0.33}MnO_3$ is accompanied by a trans-

formation of the a-b rhombuses (basal plane of the octahedra) into squares, the ''effective'' or approximate local symmetry is changing from orthorhombic to tetragonal. This change has been illustrated in Fig. 3. In the presence of isotropic Mn-O lengths, the preferential orientation of the partially occupied $d_{3z^2-r^2}$ bonds should be lost, and consequently the superexchange mechanism would not give ferromagnetic planes. The experimental observation of ferromagnetic coupling is, therefore, a strong indication against superexchange in these oxides, in consistence with the DE picture. Further investigations are necessary to assess the relevance of dynamic effects, evidenced by observation of motional narrowing[11] in $La_{2/3}Ca_{1/3}MnO_3$, upon the static description given in Table I.

Finally, apart from the fact that an isotropic basal Mn-O length below T_{IM} precludes the usual exchange coupling, a central result is our finding that the main structural modification accompanying the insulator-to-metal transition is a sudden drop of the Q_2-like cooperative deformation (Fig. 3) in the MnO_6 octahedra. It is noteworthy that this result supports recent density-functional calculations within the local spin-density approximation,[16] whose conclusion is that the basal-plane distortion mode Q_2 is, among the present symmetry breaking JT modes, responsible for the gap opening.

In conclusion, we have observed anisotropic modifications of the Mn-O bond lengths at T_{IM} which result in *a reduction of the Jahn-Teller distortion* when the system becomes ferromagnetic and metallic. These findings, very different from a mere Mn-O bond contraction associated with the metallic nature of the bond, give evidence of an electronic reorganization, and confirm the key role of the Jahn-Teller deformation in the lattice anomalies at T_{IM}. Neutron data reveal a persistent, although reduced, JT distortion above T_{IM}, reminiscent of that in the undoped manganites, in which the presence of MnO_6 units with rhombically deformed MnO_6 basal planes may indicate a residual alternating ordering in the orientation of the Mn $d_{3z^2-r^2}$ orbitals and, hence, ferromagnetic DE could coexist with antiferromagnetic (or ferromagnetic in the basal plane) superexchange interactions up to considerable doping levels. Significantly, *the residual Q_2-type basal-plane distortion vanishes at the transition*, giving more perfect octahedra with MnO_4 equatorial square planes. This observation rules out any possible ferromagnetic contribution due to simple superexchange and gives experimental support to the double-exchange picture.

We would like to acknowledge financial support by the CICYT-MIDAS (MAT94-1924-CO2), DGICYT(PB92-0849) projects and the Generalitat de Catalunya (GRQ95-8029). We thank X. Obradors for stimulating discussions. M.S. is grateful to the Instituto de Cooperación con el Mundo Arabe for a grant. The L.L.B. and the EC HCM program (Contract No. ERBCHGECT 920001) are acknowledged for making available the neutron beam time.

[1] J. B. Goodenough, Phys. Rev. **100**, 564 (1955); **124**, 573 (1961).
[2] R. von Helmolt *et al.*, Phys. Rev. Lett. **71**, 2331 (1993); Y. Tomioka *et al.*, *ibid.* **25**, 5108 (1995); P. Schiffer *et al.*, *ibid.* **18**, 3336 (1995).
[3] J. M. D. Coey *et al.*, Phys. Rev. Lett. **75**, 3910 (1995); M. F. Hundley *et al.*, Appl. Phys. Lett. **67**, 860 (1995).
[4] J. Fontcuberta, B. Martínez, A. Seffar, S. Piñol, J. L. García-Muñoz, and X. Obradors, Phys. Rev. Lett. **76**, 1122 (1996); Europhys. Lett. **34**, 379 (1996).
[5] P. G. Radaelli *et al.*, Phys. Rev. Lett. **75**, 4488 (1995).
[6] M. R. Ibarra, P. Algarabel, C. Marquina, J. Blasco, and J. García, Phys. Rev. Lett. **75**, 3541 (1995).
[7] H. Y. Hwang *et al.*, Phys. Rev. Lett. **75**, 914 (1995).
[8] J. Kanamori, J. Appl. Phys. Suppl. **31**, 149 (1960).
[9] S. Satpathy *et al.*, Phys. Rev. Lett. **76**, 960 (1996).
[10] P. Norbi *et al.*, J. Solid State Chem. **119**, 191 (1995).
[11] G. Matsumoto, J. Phys. Soc. Jpn. **29**, 615 (1970); Z. Jirák *et al.*, J. Magn. Magn. Mater. **53**, 153 (1985).
[12] J. Fontcuberta *et al.*, Solid State Commun. **97**, 1033 (1996); J. Appl. Phys. **79**, 5182 (1996).
[13] J. Rodríguez-Carvajal, Physica B **192**, 55 (1993).
[14] A. J. Millis, B. I. Shraiman, and R. Mueller (unpublished).
[15] J. L. García-Muñoz *et al.*, Phys. Rev. B **46**, 4414 (1992).
[16] H. Röder *et al.*, Phys. Rev. Lett. **76**, 1356 (1996).